Highly sensitive optical immunosensor for bacteria detection in water

ISSAM HADDOUCHE[a], LYNDA CHERBI[a], ANJAN BISWAS[b,*]
[a] *Laboratory of Instrumentation, Electronics and Computer Science Faculty, University of Sciences and Technology Houari Boumediene, Algiers, Algeria*
[b] *Operator Theory and Applications Research Group, Department of Mathematics, Faculty of Science, King Abdulaziz University, PO Box-80203, Jeddah-21589, Saudi Arabia*

In this paper a novel and highly sensitive immunosensor for bacteria detection in water based on a photonic crystal optical fiber is presented. The presented sensor is an evanescent wave type. High sensitivity (5 $\times 10^{-10}$RIU (11 cells/cm²)) is obtained with enhancing the evanescent field intensity near the sensing region by using a careful material selection and a precise geometry design of the photonic crystal fiber (PCF).

(Received March 25, 2016; accepted February 10, 2017)

Keywords: Photonic crystal fibers, Biosensors, Immunosensors, Bacteria detection E.coli, Full-Vector Finite Element Method

1. Introduction

Water analysis is important as life itself, when coming to drinking water, bacteria presence may threaten human life. Most conventional bacteriological water analyses are based on culture methods which take a long time before getting results. Rapid, portable and highly sensitive methods for pathogenic organisms detection are necessary in order to response properly to pathogenic infections [2].

During the Past decade, Photonic crystal fibers technology earned more attention in biosensing applications field, beside advantages that conventional optical fibers present such as flexibility, small size, robustness, EMI immunity and ability for remote monitoring, PCFs offer more design flexibility and possibility of greater wave field profile control thanks to the various influential geometry parameters, they also can be made of one material, even more they provide the possibility of guiding light in a hollow core [3]. In this work, the design of a PCF based immunosensor for bacteria detection in water is presented. The immunosensor's performance is improved by the fiber's geometry parameters. The sensor's design is characterized by the intensity of the evanescent part of the optical field near the sensing region, i.e the propagating light inside the fiber can interact with analytes within the penetration depth of the wave [4]. Sensor's sensitivity is directly related to the evanescent field intensity.

A precise design of the fiber's geometry is critical in order to meet some requirements such as making the fiber single mode and improving the evanescent field optical power [1]. Indeed the PCF's guiding properties is directly affected by light's wavelength, the distribution of air holes over the fiber's cross section, the size of air holes and the hole to hole pitch.

The sensor's performance is verified through Full-Vector Finite Element Method. The scope of the modeling refers to enhance sensitivity of the fiber sensor by trying to find the optimal values of the fiber's geometric parameters and making a good selection of used materials.

2. Theory

Photonic crystal fibers are a special type of optical fibers where multiple air holes arrays run inside a solid material along the waveguide axis, Fig. 1.

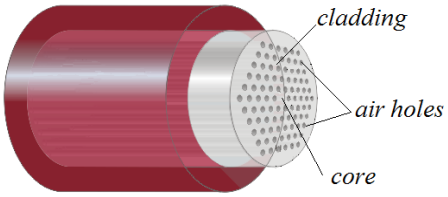

Fig. 1. Photonic crystal fiber structure

These air holes are meant to decrease the cladding's refractive index to maintain guiding inside a solid core by total internal reflection (TIR). Guidance can also be made inside a hollow core by photonic band gap (PBG). Unlike conventional optical fibers (COF), PCFs offer a large single mode wavelength range, this capability is very important in sensing applications as it allows operation at relatively high wavelengths (wider effective mode area) under single mode guiding. PCFs also offer the possibility of more manipulation of the different physical phenomena taking place inside waveguides (dispersion, non-linear effects…) [11, 18, 19]. PCF technology has opened new

perspectives to chemical-biosensing applications with all the advantages they offer.

Selectivity is a very important factor in immunosensing applications, it describes how specific antibodies are against target analytes. Antibodies are naturally made in the bodies of living species for defense against foreign microorganisms. The highly specific bio-recognition property of antibody with antigen has made it one of the most indispensable molecules for broad applications [5]. The selection of a suitable antibody is essential in immunosensing applications.

Despite the long assay time, culture based methods are still considered as the gold standard [5, 6]. Though antigen-antibody reactions are considered as the most rapid bacteria detection techniques [5], they are usually employed only to confirm the results of other methods [6, 7].

In biosensing applications PCFs are sometimes used by inserting materials (liquids or gases) inside air holes, this way offers better light-analyte interaction which will eventually enhances sensitivity, but it also requires some cumbersome procedures regarding the injection of analytes inside air holes. Recently, surface plasmon resonance (SPR) became widely used in PCF biosensing applications because of its high sensitivity, however this method suffers from various shortcomings such as the necessity of using some costly metals, the interrogation procedure required before obtaining the final results and the spectral manipulation in the case of wavelength interrogation. This will lead to a higher fabrication cost and to a longer measuring time.

By simply immobilizing analytes on the outer surface of the fiber, as illustrated in Fig. 2, and trying to enhance the evanescent power, one can get a better resolution than that obtained with SPR sensors. This makes the sensing process much simpler by just dipping the PCF sensor into substances to be analyzed.

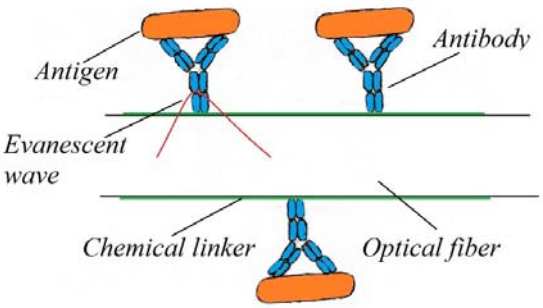

Fig. 2. Schematic diagram showing an optical fiber Immunosensor

The sensing principle of the proposed sensor is related to refractive index change of the biosensitive layer induced by antigen (bacteria cell) being bound to the immobilized antibodies on the PCF's external surface. This will lead to a variation of the effective index, hence a phase shift of the propagating wave which can be detected by an interferometer as illustrated in Fig. 3.

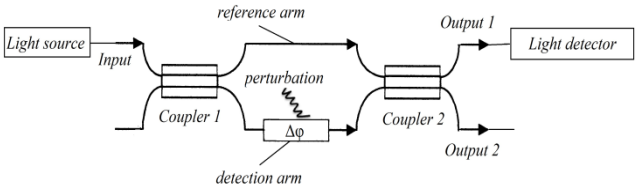

Fig. 3. Configuration of a fiber optic Mach-Zehnder Interferometer

This phase shift depends on how strong the evanescent field is. The optimal design is achieved by finding the right combination of the PCF's different geometry parameters, and this is the design that achieves the highest evanescent field intensity.

Because of the inhomogeneous nature of the cladding, PCFs cannot be studied using conventional analytical methods, so numerical methods are used.

The Full-Vector Finite Element Method is one of the most widely used techniques in optical fiber analysis. This method consists of dividing the fiber's cross section into a finite number of elements and studying and characterizing each element separately and then summing-up all elements in one global matrix. Using Maxwell's equations the following vectorial equation is derived:

$$\nabla \times (\mu_r^{-1} \nabla \times E) - k_0^2 \varepsilon_r E = 0 \qquad (1)$$

Where E is the electric field, k_0 is the wave number, ε_r and μ_r are the relatives permittivity and permeability respectively.

3. Results and discussion

The proposed photonic crystal fiber sensor is shown in Fig. 4. This design consists of solid core index-guiding PCF with two rings of air holes arranged in hexagonal-lattice distribution and a central air hole in the core helping to extend the electric field toward the sensitive region. The holes in the second ring are made smaller in order to allow more optical power to pass through and thus achieving the best interaction between the evanescent field and analytes. The biosensitive layer consists of the immobilizing material i.e. chemical linker (ex: mercapto undecanoic acid), and capture antibodies.

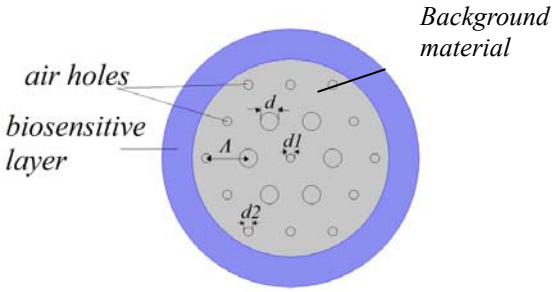

Fig. 4. Geometry of the proposed sensor

In this study two models of PCF immunosensor are compared in order to examine the performance of this sensor, where the background material of the PCF in the first model is made of silica, while in the second model it is made of polydimethylsiloxane, PDMS (Sylgard 184).

The numerical values of the geometric parameters of this PCF-sensor are: $\Lambda=2.1\mu m$, $d=0.9\mu m$, $d_1=0.4\mu m$, $d_2=0.45\mu m$, PCF's radius $R = 4.9\mu m$ and PCF's length $L=5cm$.

Silica, PDMS and water are modeled using Sellmeier equation [12, 13, 14]:

$$n(\lambda)^2 = 1+\frac{B_1\lambda^2}{\lambda^2-C_1}+\frac{B_2\lambda^2}{\lambda^2-C_2}+\frac{B_3\lambda^2}{\lambda^2-C_3} \quad (2)$$

The following figure depicts the calculated refractive index perturbation Δn_b at the biosensitive layer as a function of bacteria density on the external surface of the proposed sensor, where E.coli was taken as an example, E.coli cells are considered as rod like cells with a half-length a = 1µm and a radius b = 0.4µm, having an average refractive index n=1.366 at a wavelength λ = 1.31µm [15]. Δn_b is assumed to vary linearly with the volume ratio between bacteria cells and the biosensitive layer.

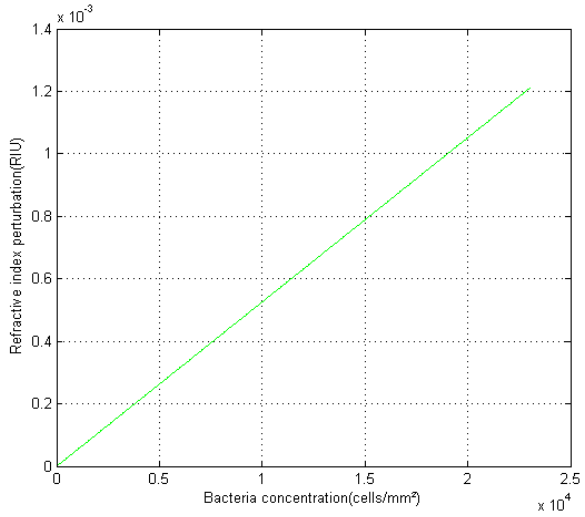

Fig. 5. Refractive index perturbation plot versus bacteria density for a waveguide length L = 5cm and an operating wavelength of λ=1.311µm

Transverse electric field profiles of the fundamental mode (HE_{11}) are illustrated in Figs. 6.a and 6.b for silica and PDMS sensors respectively.

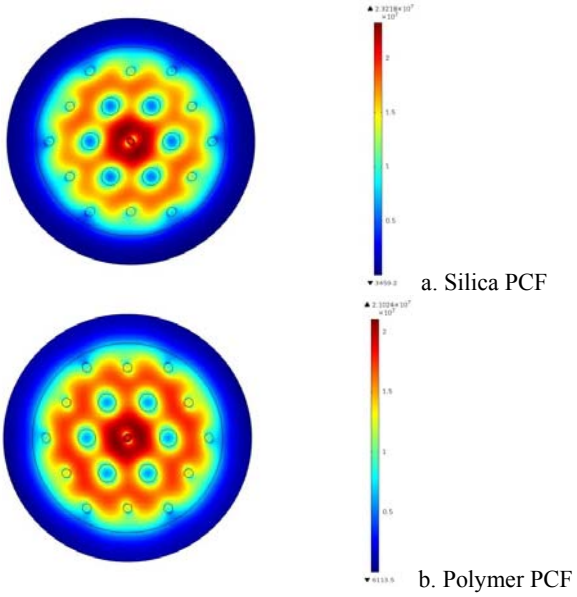

Fig. 6. Transverse electric field profile of the fundamental mode (HE_{11}) with d=0.9µm, Λ=2.1µm and λ=1.31µm

One important parameter is the effective mode area (A_{eff}), A_{eff} shows how much the wave field is extended outside the core.

Table 1 shows (A_{eff}) calculation for both sensor models for different values of d and Λ.

A_{eff} is calculated by means of the following equation [9]:

$$A_{eff} = \frac{\left(\iint_S |E_t|^2\, dxdy\right)^2}{\iint_S |E_t|^4\, dxdy} \quad (3)$$

Where E_t is the transverse component of the electric field.

Table 1. Effective mode area calculation results for different values of d and Λ.

	Hole diameter d (µm)	*Hole to hole pitch Λ (µm)*	*Effect mode area A_{eff} (μm^2)*
Silica Sensor	*0.9*	*2.1*	*55.86*
	1	*2.2*	*50.65*
	1.1	*2.3*	*41.17*
Polymer Sensor	*0.9*	*2.1*	*62.91*
	1	*2.2*	*58.98*
	1.1	*2.3*	*51.37*

Table 1 shows how much sensor's performance is affected by the PCF's geometry parameters, it clearly illustrates the dependence of the mode field profile on the hole diameter (d) and hole to hole pitch (Λ), the effective mode area is inversely proportional to d/Λ ratio, this is due to the fact that the mode field diameter (MFD) is inversely proportional to refractive index contrast Δn between the core and the cladding [9, 10].

A_{eff} is more important in Polymer PCF than in Silica PCF, this is because $\Delta n_{PDMS\ \mathrm{pcf}} < \Delta n_{\ silica\ \mathrm{pcf}}$ (refractive index of PDMS is lower than that of silica), this explains why the mode field profile seems wider in the PDMS sensor.

Other results are reported in Table 2, where effective mode area A_{eff} and the loss ratio Γ are calculated for three different wavelength values (λ). Γ is the ratio between the evanescent optical power radiated outside the waveguide and the total optical power.

$$\mathrm{r} = \frac{P_r}{P_t}\% \tag{4}$$

Table 2. Effective mode area and loss ratio for different values of wavelength, d =0.9μm and Λ=2.1μm.

	Wavelength λ(μm)	Effective mode area A_{eff} (μm²)	Loss ratio Γ (%)
Silica Sensor	*0.5*	*43.52*	*0.04*
	1.0	*48.87*	*0.32*
	1.55	*55.86*	*1.11*
Polymer Sensor	*0.5*	*45.01*	*0.09*
	1.0	*53.48*	*0.8*
	1.55	*62.91*	*2.48*

According to Table 2, loss ratio is more important in PDMS PCF sensor, this is because the refractive index contrast between the sensitive region and the background material of the PCF is lower in PDMS sensor case, which leads to more penetration of the optical field into the sensitive region.

Both parameters A_{eff} and Γ increase with wavelength, this is because the MFD is directly proportional to λ [9, 10].

The sensitivity of the proposed sensor is calculated by evaluating the phase shift in the propagating wave induced by bacteria presence,

$$\Delta\emptyset = \frac{2\pi}{\lambda} L\, \Delta n_{eff} \tag{5}$$

$$S = \frac{d\emptyset}{dn_b} = \frac{2\pi}{\lambda} L\, \frac{dn_{eff}}{dn_b} \tag{6}$$

Where $\emptyset$, L, n_{eff}, n_b are the phase of the propagating mode, the length of the PCF, the effective index of the propagating mode and the refractive index of the biosensitive layer.

In Figs. 7 and 8, sensitivity S[rad/RIU] is plotted versus bacteria density [cells/mm²] and wavelength λ[μm] respectively.

It is obvious from both graphs that the PDMS sensor is more sensitive to refractive index perturbation than silica sensor, this agrees with the results obtained in Table 2 where it was found that the energy radiated outside the waveguide i.e. energy interacting with analytes, is more important in PDMS sensor In Fig. 7, as bacteria density increases the sensor becomes more sensitive, this is explained by the decrease of refractive index contrast between the waveguide and the biosensitive layer allowing more energy to penetrate inside the biosensitive layer.

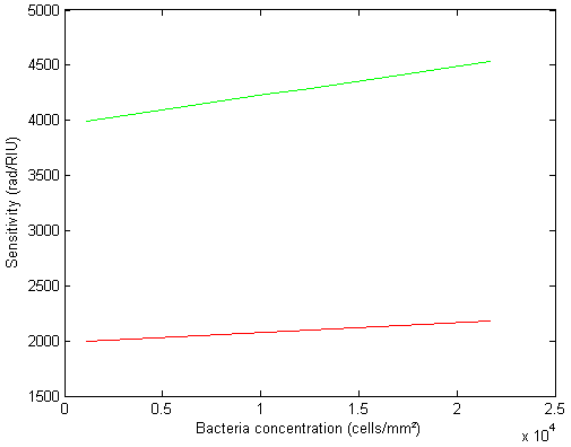

Fig. 7. Sensitivity plot versus bacteria density for silica sensor (red) and PDMS sensor (green) with d = 0.9μm, Λ=2.1μm, λ = 1.31μm

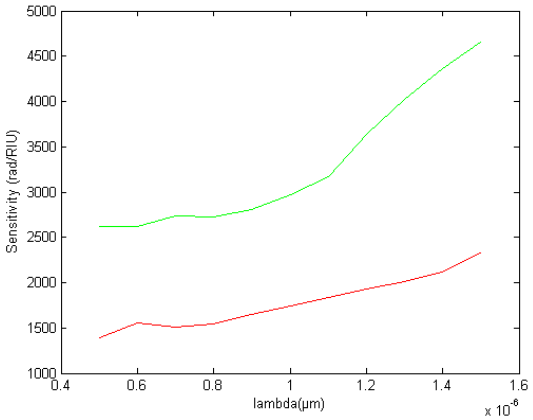

Fig. 8. Sensitivity plot versus operating wavelength for silica sensor (red) and PDMS sensor (green) with d = 0.9μm and Λ=2.1μm

Despite the $\frac{1}{\lambda}$ term in equation (6) the increase rate of sensitivity with wavelength is remarkably important in Fig. 8, this also agrees with the previous results, where the influence of the wavelength on the mode field profile was proved to be very important.

If we assume that a Mach-Zhender interferometer can reliably detect a 10^{-6} rad phase shift [16] this results in a sensor resolutions of 2.53×10^{-10} RIU (5 cell/cm²) and 5×10^{-10} RIU (11 cells/cm²) for PDMS and silica sensors respectively at an operating wavelength λ=1.31μm, these results are much better than those reported in [15,17].

If we want to test the designed sensor and use it in an interferometer configuration we should take into

consideration different sources of noise such as fiber's length change with respect to temperature and strain, and also errors related to the limitations of used devices such as light detectors, all these factors affect the real resolution of the sensor.

4. Conclusion

The design of an evanescent field PCF-based immunosensor is presented in this paper. The performances of two PCF based sensors designs are compared, silica and PDMS PCF sensors.

The PDMS sensor has proved better performance over silica sensor. The detection limits of both sensors are 2.53×10^{-10} RIU (5 cells/cm²) and 5×10^{-10} RIU (11 cells/cm²) for PDMS and silica sensors respectively. However these results are to be confirmed experimentally.

This work was dedicated to bacteria detection, however it can be generalized to any bio-chemical measurements.

It is important to notify that materials absorption (imaginary part of refractive index) of light was omitted due to the short length of the sensor.

The presented sensor can be a good alternative to conventional methods for determining bacteria concentration in liquids, it is also important to note that a better enhancement can be added by trying new geometries or by using new materials.

References

[1] L. Mescia, F. Prudenzano, L. Allegretti, G. Calo, M. De Sario, A. D'Orazio, L. Maiorano, T. Palmisano, V. Petruzzelli, Journal of Non-Crystalline Solids **355**, (2009).

[2] M. Taniguchi, E. Akai, T. Koshiba, K. Hibi, H. Hudo, K. Otsuka, H. Saito, K. Yano, H. Endo, K. IFMBE Proceedings **15**, 308 (2007).

[3] Ana M. R. Pinto, Manuel Lopez-Amo, Journal of Sensors **2012**, (2012).

[4] S. Yin, C. Zhan, P. Ruffin, Fiber optic sensors (2008).

[5] P. Banada, A. Bhunia, Recognition Receptors and Microsystems, Springer Science and Business Media, LLC (2008).

[6] J. Odumeru, C. Leon-Velarde, *Salmonella* Detection Methods for Food and Food Ingredients, InTech (2012).

[7] R. Hayman, Springer Science and Business Media, LLC (2008).

[8] T. Dar, Modeling and characterization of label free optical biosensors, City University London (2013).

[9] K. Saitoh, M. Koshiba, Journal of Lightwave Technology **23**(11), 3580 (2005).

[10] G. P. Agrawal, Fiber optic communications systems, John Wiley & Sons (2002).

[11] G. P. Agrawal, Nonlinear fiber optics, Elsevier (2007).

[12] W. Qiu, PDMS Based Waveguides for Microfluidics and EOCB, A Thesis - Submitted to the Graduate Faculty of the Louisiana State University and Agricultural and Mechanical College in partial fulfillment of the requirements for the degree of Master of Science in Mechanical Engineering (2012).

[13] A. Kumar, A. Ghatak, SPIE Tutorial Texts **TT90**, Tutorial Texts in Optical Engineering, SPIE Press (2011).

[14] Y. Coello, Applied Optics **46**(35), 8394 (2007).

[15] H. Ren, Opt. Express **15**(25), 17410 (2007).

[16] M. Ferreti, Capteurs à fibres optiques, Techniques de l'ingénieur, R415 (1996).

[17] E. Akowuah, IEEE Journal of Quantum Electronics **48**(11), 1403 (2012).

[18] Rui Guo, Hui-Qin Hao, Elsevier, Annals of Physics **344**, 10 (2014).

[19] Rui Guo, Hui-Qin Hao, Commun Nonlinear Sci Numer Simulat. **18**, 2426 (2013).

*Corresponding author: biswas.anjan@gmail.com